*31st EPS Conference on Plasma Phys. London, 28 June - 2 July 2004 ECA Vol.**28G**, P-5.183 (2004)*

Tokamak turbulence computations on closed and open magnetic field lines

T. Ribeiro[1,2], B. Scott[2], D. Coster[2] and F. Serra[1]

[1] *Centro de Fusão Nuclear – EURATOM/IST Association, Av. Rovisco Pais 1, 1049-001 Lisbon, Portugal*
[2] *Max-Planck-Institut für Plasmaphysik, EURATOM Association, D-85748 Garching bei München, Germany*

Introduction A magnetic field which is doubly periodic and also generally sheared leads to the so called field line connection. This property is the reason why the parallel wavenumber $k_\parallel$ cannot vanish for finite sized fluctuations (finite $k_\perp$), since $k_\parallel = (m_0 - nq)/ \pm m'/qR$ [1], where q is the magnetic field pitch parameter, and R is the plasma major radius. On the other hand, in the scrape-off layer (SOL), the field lines end on plates, which breaks the field line connection constraints. This allows the convective cell modes – finite $k_\perp$ but zero $k_\parallel$ – to exist. We are used to two dimensional turbulence computations in the SOL [2], and three dimensional toroidal computations using closed magnetic surface geometry. The three dimensional simulation of the SOL region is starting to be addressed [3,4,5]. In this paper we study turbulence on closed and open flux surfaces in a comparative manner using the three dimensional electromagnetic gyrofluid turbulence code GEM3 [6]. The results show their distinctions and stress the importance of the field line connection for drift wave turbulence, and the implications to be expected for SOL vs. edge turbulence in the experiment.

The model The normalised equations for the two moment gyrofluid model GEM3 (similar to fluid) used in this work are (details and energetics in Ref.6), for the electrons

$$\left(\frac{\partial}{\partial t} + \mathbf{v}_E \cdot \nabla\right) \tilde{n}_e = -B\nabla_\parallel \frac{v_\parallel}{B} + \mathcal{K}(\tilde{\phi} - \tilde{n}_e) \tag{1}$$

$$\hat{\beta}\frac{\partial \tilde{A}_\parallel}{\partial t} - \hat{\mu}\left(\frac{\partial}{\partial t} + \tilde{\mathbf{v}}_E \cdot \nabla\right) \tilde{v}_\parallel = -\nabla_\parallel \left(\tilde{\phi} - n_e\right) + \hat{\mu}\mathcal{K}(2\tilde{v}_\parallel) - C\tilde{J}_\parallel \tag{2}$$

and for the ions

$$\left(\frac{\partial}{\partial t} + \mathbf{u}_E \cdot \nabla\right) \tilde{n}_i = -B\nabla_\parallel \frac{u_\parallel}{B} + \mathcal{K}(\tilde{\phi}_G + \tau_i\tilde{n}_i) \tag{3}$$

$$\hat{\beta}\frac{\partial \tilde{A}_\parallel}{\partial t} + \hat{\varepsilon}\left(\frac{\partial}{\partial t} + \tilde{\mathbf{u}}_E \cdot \nabla\right) \tilde{u}_\parallel = -\nabla_\parallel \left(\tilde{\phi}_G + \tau_i n_i\right) + \tau_i\hat{\varepsilon}\mathcal{K}(2\tilde{u}_\parallel) - C\tilde{J}_\parallel \tag{4}$$

and for polarisation and induction:

$$\Gamma_1\tilde{n}_i + \frac{\Gamma_0 - 1}{\tau_i}\tilde{\phi} = \tilde{n}_e \qquad\qquad -\nabla_\perp^2 \tilde{A}_\parallel = \tilde{J}_\parallel = \tilde{u}_\parallel - \tilde{v}_\parallel \tag{5}$$

where $C = (0.51\nu_e L_\perp/c_s)(m_e/M_i)(qR/L_\perp)^2$ is the drift wave collisionality parameter, $L_\perp$ is the profile gradient scale, $\tau_i = T_i/T_e$, and $\mathbf{v}_E$ is the ExB velocity, and $\mathbf{u}_E$ is the same but with the gyroaveraged electrsotatic potential $\tilde{\phi}_G = \Gamma_1\tilde{\phi}$ [6]. The curvature operator is represented by the terms $\mathcal{K} = -\nabla\cdot(c/B^2\mathbf{B}\times\nabla)$; this and other details of the flux tube geometry can be found in reference [1].

Concerning the parallel boundary conditions, global consistency must be ensured in the closed field lines region so that $f(\theta+2\pi, \xi-2\pi q) = f(\theta,\xi)$ where θ and ζ are the geometrical poloidal and toroidal angles, respectively, and $\xi = \zeta - q\theta$ is a transformed coordinate such that (θ,ξ) form a field aligned coordinate system [7]. In the SOL region, since the field lines end on the divertor plates, this pseudo-periodicity condition no longer needs to be fulfilled. Based on Debye sheath physics, we use a standard model to specify, at the referred locations, the flux variables of GEM as functions of the state variables, namely $\tilde{u}_\parallel\big|_{\theta=\pm\pi} = \pm\Gamma_D(\tilde{p}_e)$ and $\tilde{v}_\parallel\big|_{\theta=\pm\pi} = \pm\left(\tilde{u}_\parallel\big|_{\theta=\pm\pi} - \tilde{J}_\parallel\Big|_{\theta=\pm\pi}\right) = \pm\left[\tilde{u}_\parallel\big|_{\theta=\pm\pi} - \Gamma_D\left(\tilde{\phi} - \Lambda\tilde{T}_e\right)\right]$, that is, the ion and electron parallel velocities, with the magnetic potential $\tilde{A}_\parallel$ determined via Ampere's law. In the previous expressions, it should be noted that $\Lambda = \log\sqrt{M_i/2\pi m_e} \approx 3$ and $\Gamma_D = 2\pi L_\perp/L_\parallel \ll 1$. Note also that $\tilde{p}_e = \tilde{n}_e$ (normalised) is used instead of $\tilde{T}_e$ as a working model, since the two moment model of GEM3 does not include the temperatures. The state variables, namely the electron density $\tilde{n}_e$, the ion density $\tilde{n}_i$, the electrostatic potential $\tilde{\phi}$ and the ion gyroaveraged electrostatic potential $\tilde{\phi}_G$, are obtained using Neumann boundary conditions.

Results For the closed field lines region, the three dimensional structure of the state variables show a clear indication of the field line connection, when compared to the open field lines case. In the former case, structures with finite k_y lose their identity along the field line before one field line connection is completed ($k_\parallel \neq 0$). In the later case, convective cells, structures with finite perpendicular wavelengths that exist across the whole parallel domain and extend beyond that, clear exist $k_\parallel = 0$.

Since $\tilde{\phi}$ is controlled indirectly by the resistivity $C\tilde{J}_\parallel$ through the energy transfer term $\tilde{J}_\parallel\nabla_\parallel\tilde{\phi}$ [6] and in closed field lines $k_\parallel qR = \mathcal{O}(1)$, the dissipation through the parallel dynamics is much higher in this region than in the SOL. Here, the field lines are opened, allowing $\nabla_\parallel$ to vaninsh. Futher, Γ_D provides a direct damping mechanism on $\tilde{\phi}$ of the order of $\Gamma_D/k_\perp^2$, but at much smaller levels than $(k_\parallel qR)^2C^{-1}/k_\perp^2$, since Γ_D is roughly one to two orders of magnitude smaller than C^{-1}. Hence, it is only effective for the larger perpendicular wavelenghts. Figure 1 describes the source and sink spectra, showing, the ExB gradient drive, magnetic flutter drive and the dissipation averaged over time, radial and parallel direction [6]. Plots (a) and (b) show the closed field lines and SOL cases, respectively. In the SOL, then, the reduced dissipation leads to

stronger drive, and at lower k_y. In order to assess the importance of the Debye sheath losses on the turbulence, an alternative "zero loss" model was also used, setting the Debye fluxes to zero by setting $\Gamma_D = 0$ in the sheath model. With the direct damping on $\tilde{\phi}$ removed the low k_y modes can now grow uninhibited, due to the inverse ExB energy cascade, as is clearly seen in plot (c) of the same figure. That leads to the low k_y mode domination characteristic of interchange turbulence. The constraints imposed to the amplitudes of $\tilde{\phi}$ therefore relax as the parallel dissipation is decreased. This is also seen in the next diagnostic (figure 2), which plots the parallel structure of the amplitudes of the $\tilde{\phi}$, $\tilde{n}_e$ and $\tilde{h}_e = \tilde{\phi} - \tilde{n}_e$. The uninhibited growth of $\tilde{\phi} \gg \tilde{n}_e$ in the zero loss case is clear. In closed field lines, the controlling mechanism for $\tilde{\phi}$ keeps it at a value closer to $\tilde{n}_e$ Figure 3 shows the phase shift (α) distribution of $\tilde{n}_e$ ahead of $\tilde{\phi}$. For closed field lines, $0 < \alpha < \pi/2$, which is typical of drift wave type turbulence. The part of the spectra with the larger values of α are due to the collisionality. For the zero loss case, α is closer to $\pi/2$ and the SOL case stays in between. It is noteworthy that, with the Debye losses, the phase shifts at low k_y are lower, the reason being that is where the dissipation through Γ_D is most effective.

Outline These results show the impact of parallel dynamics and field line connection on the turbulence. The transition between closed and open field lines revealed the fundamental difference between the edge and the SOL regions of the plasma. The fact that convective cells are allowed outside the last closed flux surface, and not inside, changes the turbulence in the SOL to an interchange type. The transport is also affected as a consequence of the decreased parallel dissipation on $\tilde{\phi}$ which happens when $k_{\|} qR \ll 1$. These signatures should be observable in experiment.

Acknowledgments This work, supported by the European Communities and "Instituto Superior Técnico", has been carried out within the Contract of Association between EURATOM and IST. Financial support was also received from "Fundação para a Ciência e Tecnologia" in the frame of the Contract of Associated Laboratory.

References

[1] B. Scott, *Phys. Plasmas* **8** (2001) 447
[2] P. Beyer, Y. Sarazin, X. Garbet et al, Plasma Phys. Contr. Fusion **41** (1999) A757.
[3] B. Scott, *23rd EPS Conf. on Control. Fusion Plasma Phys.* **A005** (1996) 54
[4] X. Xu, R. Cohen, T. Rognlien, J. Myra, Phys. Plasmas **7** (2000) 1951.
[5] V. Naulin, et. al, (arXiv:physics/0309015 v1, Sep 2003)
[6] B. Scott, *Plasma Phys. Control. Fusion* **45** (2003) A385
[7] B. Scott, *Phys. Plasmas* **5** (1998) 2334

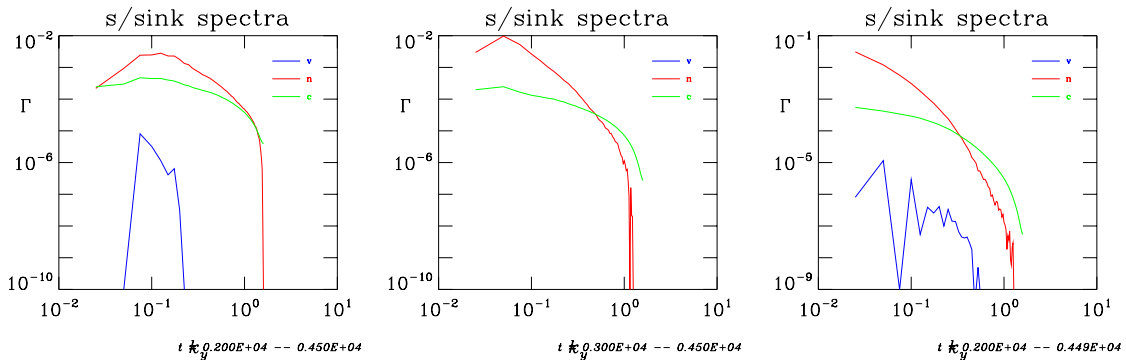

Figure 1: Transport spectra showing the magnetic flutter drive ('v' – blue), the ExB gradient drive ('n' – red) and dissipation ('c' – green) for the (a) closed field lines case, (b) Debye sheath model and (c) zero flux model. Note that in all figures presented, we use the coordinates y and s correspond to a rescalling of the previous mentioned coordinates ξ and θ, respectively [1].

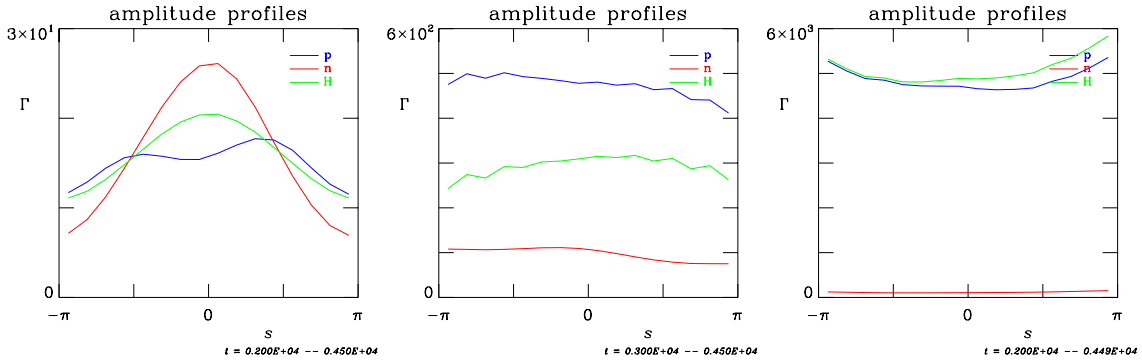

Figure 2: Envelopes of the squared amplitudes of $\tilde{\phi}$ ('p' –blue), $\tilde{n}_e$ ('n' – red) and $\tilde{h}_e = \tilde{\phi} - \tilde{n}_e$ ('H' – green), as functions of the parallel coordinate, with (a), (b) and (c) as in figure 1.

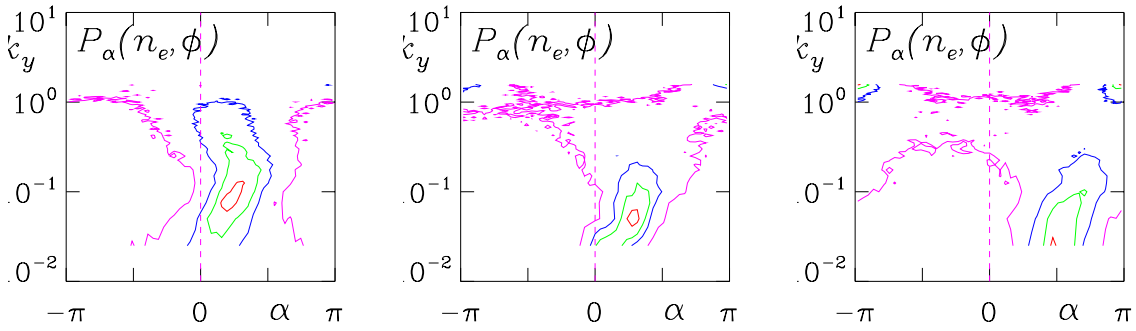

Figure 3: Phase distributions of $\tilde{n}_e$ ahead of $\tilde{\phi}$ at each k_y. (a), (b) and (c) like before